Jong Min Lee[1]*
Ji-eun Kim[1]*
Edward Kang[2]
Sang-Hoon Lee[2]**
Bong Geun Chung[1]

[1]Department of Bionano Engineering, Hanyang University, Ansan, Korea
[2]Department of Biomedical Engineering, Korea University, Seoul, Korea

Received March 14, 2011
Revised May 3, 2011
Accepted May 3, 2011

Short Communication

An integrated microfluidic culture device to regulate endothelial cell differentiation from embryonic stem cells

We developed an integrated microfluidic culture device to regulate embryonic stem (ES) cell fate. The integrated microfluidic culture device consists of an air control channel and a fluidic channel with 4×4 micropillar arrays. We hypothesized that the microscale posts within the micropillar arrays would enable the control of uniform cell docking and shear stress profiles. We demonstrated that ES cells cultured for 6 days in the integrated microfluidic culture device differentiated into endothelial cells. Therefore, our integrated microfluidic culture device is a potentially powerful tool for directing ES cell fate.

Keywords:
Embryonic stem cell / Endothelial cell differentiation / Integrated microfluidic device
DOI 10.1002/elps.201100161

Embryonic stem (ES) cells, which are pluripotent cells derived from the inner cell mass of a blastocyst, play an important role in studying regenerative medicine [1–4]. In particular, endothelial cell differentiation derived from ES cells is of great interest in understanding vascular regeneration processes, such as vasculogenesis and angiogenesis [5–7]. A hydrogel microwell array system has been previously developed to study endothelial cell differentiation from ES cells [8]. This system promoted the formation of uniform-sized embryoid bodies (EBs), which were spontaneously aggregated to form three-germ layers. It demonstrated that ES cell-derived endothelial cells were highly expressed in smaller EBs and this vascular behavior was strongly regulated by WNT5a signaling.

Integrated microfluidic platforms containing pneumatically actuated microvalves have been recently developed to direct ES cell fate [9–12]. For instance, the gene expression of single human ES cells has been investigated in an integrated microfluidic device, in which nanoliter amounts of soluble factors can be manipulated [9]. To synthesize cDNA, mRNA of single ES cells was extracted from the integrated microfluidic device. The mRNA-to-cDNA conversion efficiency was five times higher as compared with conventional methods. A real-time microfluidic system has also been developed to culture mouse ES cells in a 3-D environment [10]. In this system, pneumatically actuated ring-shaped microvalves were integrated in the microfluidic device to enable real-time control of the delivery of soluble factors. Computational fluid dynamic calculations revealed that the flow rate increased with increasing conduit height in the 3-D extracellular matrix environment. Fluorescent images indicated that mouse ES cells that were encapsulated within 3-D Matrigels showed self-renewal for 5 days in the integrated microfluidic device. Therefore, the integrated microfluidic device is a potentially powerful tool for controlling the proliferation and pluripotency of ES cells. Despite the potential of integrated microfluidic devices, previous integrated microfluidic systems have some limitations, such as the system is complicated to culture ES cells and ES cell differentiation has not been fully explored in integrated microfluidic devices.

The microfluidic perfusion devices with circular microchambers have also been developed for cell culture and medium perfusion [13, 14]. The cells were cultured within circular microchamber arrays and their growth rate was investigated in response to the perfusion rate. Furthermore, microfluidic culture platforms containing multi-layer arrays [12], microwells [15], and polycarbonate membranes [16] have been previously developed for ES cell docking, growth, and differentiation. However, these microfluidic devices have been used for controlling uniform

Correspondence: Professor Bong Geun Chung, Department of Bionano Engineering, Hanyang University, Ansan, Korea
E-mail: bchung@hanyang.ac.kr
Fax: +82-31-436-8153

Abbreviations: EBs, embryoid bodies; **EGM-2,** endothelial growth medium-2; **ES,** embryonic stem

*These authors contributed equally to this work.
**Additional corresponding author: Professor Sang-Hoon Lee
Email: dbiomed@korea.ac.kr

Colour Online: See the article online to view Figs. 1–3 in colour.

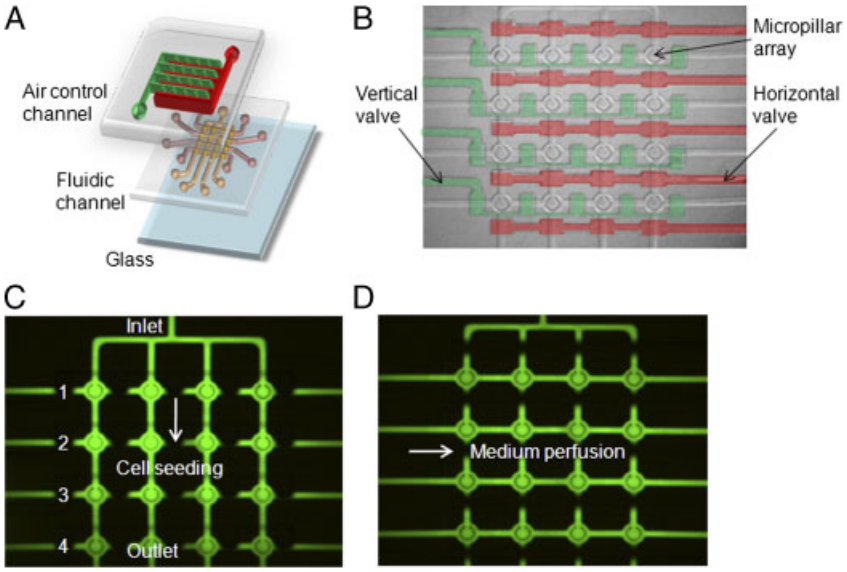

Figure 1. Integrated microfluidic culture device. (A) Schematic of the integrated microfluidic culture device containing a fluidic channel and an air control channel. (B) 4×4 integrated microfluidic culture device with horizontal and vertical valves. (C and D) Fluorescent images of microvalves that can actuate for cell seeding and medium perfusion.

EB sizes and EB-derived differentiation. As compared with the previously developed microfluidic devices, our integrated microfluidic device has several advantages, such as shear-protective micropillar arrays for uniform single ES cell docking and ES cell-derived endothelial cell differentiation, valve-controlled cell seeding and medium perfusion system. Furthermore, the effect of the microscale post distance on velocity profile and shear stress within micropillar arrays is investigated.

To culture ES cells, we developed a 4×4 integrated microfluidic device containing an air control channel and a fluidic channel with 4×4 micropillar arrays (300 μm in diameter) (Fig. 1A and B) (see Materials and Methods of Supporting Information). Microscale posts (12 μm distance between the posts) were placed within the micropillar arrays to facilitate the ES cell docking. We hypothesized that ES cells would be docked within the micropillar arrays and medium could be perfused into the micropillar array. We also actuated microvalves in a sequential manner for ES cell seeding and medium perfusion in our integrated microfluidic device (Fig. 1C and D).

To predict the velocity profile within the micropillar arrays, we simulated the computational fluid dynamics of the velocity profile using FEMLAB software (Fig. 2A) (see Materials and Methods of Supporting Information). The computational fluid dynamic simulations showed that the velocity profiles were strongly affected by the distance between the posts (i.e. 12, 42, and 96 μm) within the micropillar arrays. The velocity profiles did not penetrate into the micropillar arrays when the distance between the posts was narrow (12 μm), whereas the velocity profiles penetrated into the micropillar arrays when the distance between the posts was 96 μm. We also simulated the shear stress profiles within the micropillar arrays (Fig. 2B). Similar to the modeling results of the velocity profile, the shear stress profiles were also strongly affected by the distance between the posts within the micropillar arrays, showing that micropillar arrays containing posts spaced 12 μm apart were shear-protective. The shear stress modeling analysis revealed that the shear stress profiles were linearly proportional to the flow velocity (Fig. 2C). To control the shear stress profiles within micropillar arrays containing posts spaced 12 μm apart, we also optimized the shapes (i.e. circle, triangle, and quadrangle) of the microscale post (Fig. 2D). It was revealed that microscale posts with the quadrangular shapes showed more shear-protective as compared with circular and triangular shapes. Furthermore, we hypothesized that microparticle tracking simulations would predict cell docking within the micropillar arrays (Fig. 2E). As expected, the numbers of particles entrapped within micropillar arrays increased linearly with the numbers of particles seeded into the micropillar arrays. This computational modeling approach allows optimization of cell seeding density to regulate uniform cell docking within the micropillar arrays. However, it should be noted that particle tracking simulations may not accurately reflect the actual cell docking behavior, because the properties of particles are not identical to those of cells.

After theoretical analysis of numbers of the particles that could be entrapped within the micropillar arrays, we investigated cell docking within micropillar arrays containing posts separated by 12 μm (Fig. 2F). ES cell docking was controlled by the flow rate (1-10 μL/min). Arrays 1 and 4 are the micropillar arrays that are close to the cell seeding inlet and outlet, respectively (Fig. 1C). Quantitative analysis demonstrated that the numbers of cells docked within the micropillar arrays decreased with increasing flow rate. We found that 35–52 cells were docked within micropillar arrays at a flow rate of 1 μL/min, whereas only 7–12 cells were entrapped within the micropillar arrays at a flow late of 10 μL/min. Interestingly, we observed that faster flow rates (5, 10 μL/min) enabled more uniform ES cell docking than a

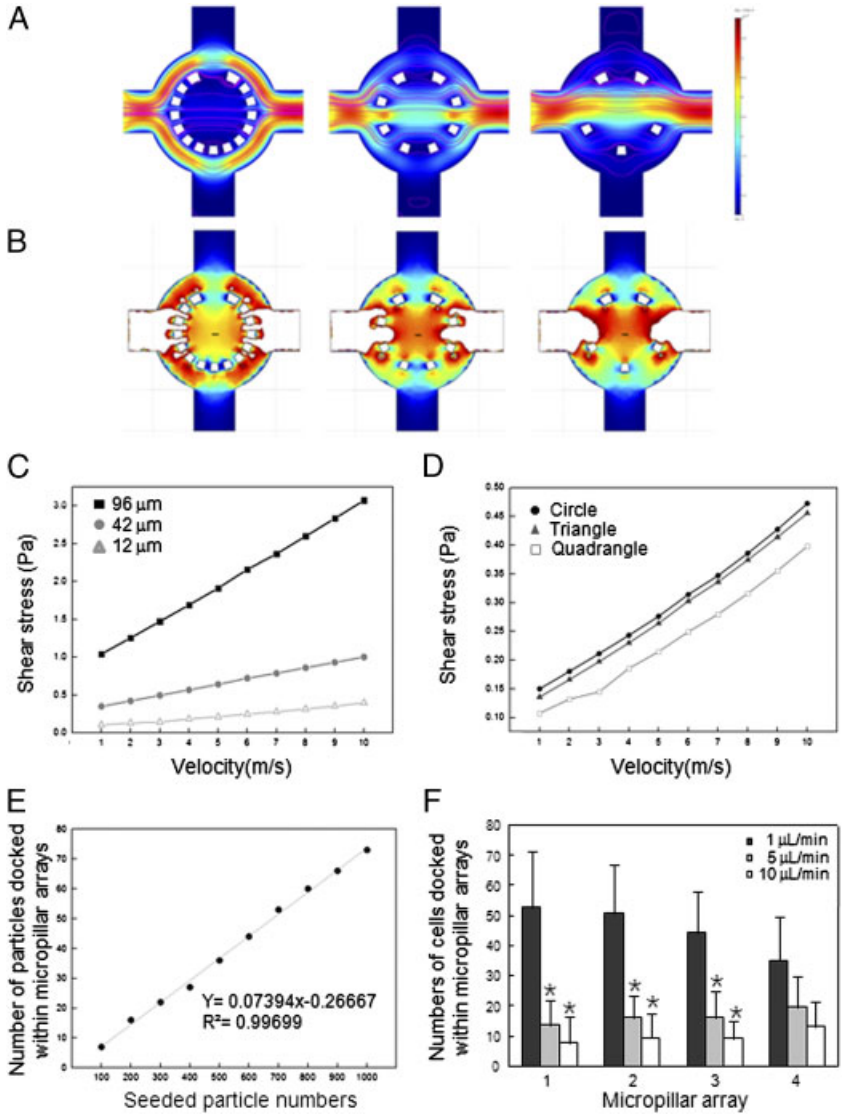

Figure 2. Analysis of the velocity profile, shear stress, and cell docking within micropillar arrays. (A) Modeling of velocity profiles. (B) Shear stress profiles on the bottom substrate of *X*-axis within the micropillar array with respect to the distance (12, 42, and 96 μm) between the posts (3×10^{-5} m/s average inlet velocity). (C) Analysis of shear stress profiles in the micropillar arrays in response to fluidic velocity (3×10^{-5} m/s average inlet velocity). (D) Analysis of shear stress profiles in micropillar arrays containing various shapes (i.e. circle, triangle, and quadrangle) of the microscale posts. (E) Analysis of the numbers of particles docked within the micropillar arrays (3×10^{-5} m/s average inlet velocity). (F) Quantitative analysis of cell docking inside the micropillar arrays of the integrated microfluidic culture device. Cell docking was highly dependent on the flow rate (1–10 μL/min). Arrays 1 and 4 of the micropillar were close to the cell seeding inlet and outlet, respectively ($^*p < 0.05$).

slower flow rate (1 μL/min). The maximum number of cells docked within a micropillar array was approximately 52 in array 1, when a flow rate of 1 μL/min was used. The minimum number of cells docked within a micropillar array was 7 in array 1 at a flow rate of 10 μL/min. Therefore, we optimized the flow rate (5–10 μL/min) to achieve uniform cell docking within the micropillar arrays.

To further study the ES cell-derived endothelial cell differentiation, ES cells were cultured for 6 days with 50% EB medium and 50% endothelial growth medium-2 (EGM-2) in our integrated microfluidic culture device (Fig. 3). ES cells were also cultured simultaneously in six-well plates with 100% EB medium (Fig. 3A) or a mixture of 50% EB medium and 50% EGM-2 medium (Fig. 3B). Fluorescent images showed that ES cells cultured with 50% EB medium and 50% EGM-2 differentiated to a greater extent into endothelial cells than cells cultured in 100% EB medium. ES cell-derived endothelial cell differentiation was confirmed by staining for the endothelial marker (anti-platelet endothelial cell adhesion molecule, PECAM; green). Immunocytochemistry showed that ES cells were uniformly docked within the 4×4 micropillar arrays of the integrated microfluidic culture device (Fig. 3C). Furthermore, ES cells cultured in the integrated microfluidic culture device did not aggregate in contrast to the ES cells cultured in six-well plates. This difference is probably due to the continuous perfusion of medium in the microfluidic device, which would remove molecules secreted by the ES cells. However, the shape (i.e. round single cells) of ES cell-derived endothelial cells in the integrated microfluidic culture device (Fig. 3D) was similar to the shape of cells cultured in six-well plates (Fig. 3B, see high-magnification image). Quantitative analysis showed that ES cells cultured for 6 days in the integrated microfluidic device were more differentiated into PECAM-positive endothelial cells (90%) (Fig. 3E). Furthermore, we are now performing high-throughput experiments using various soluble factors to

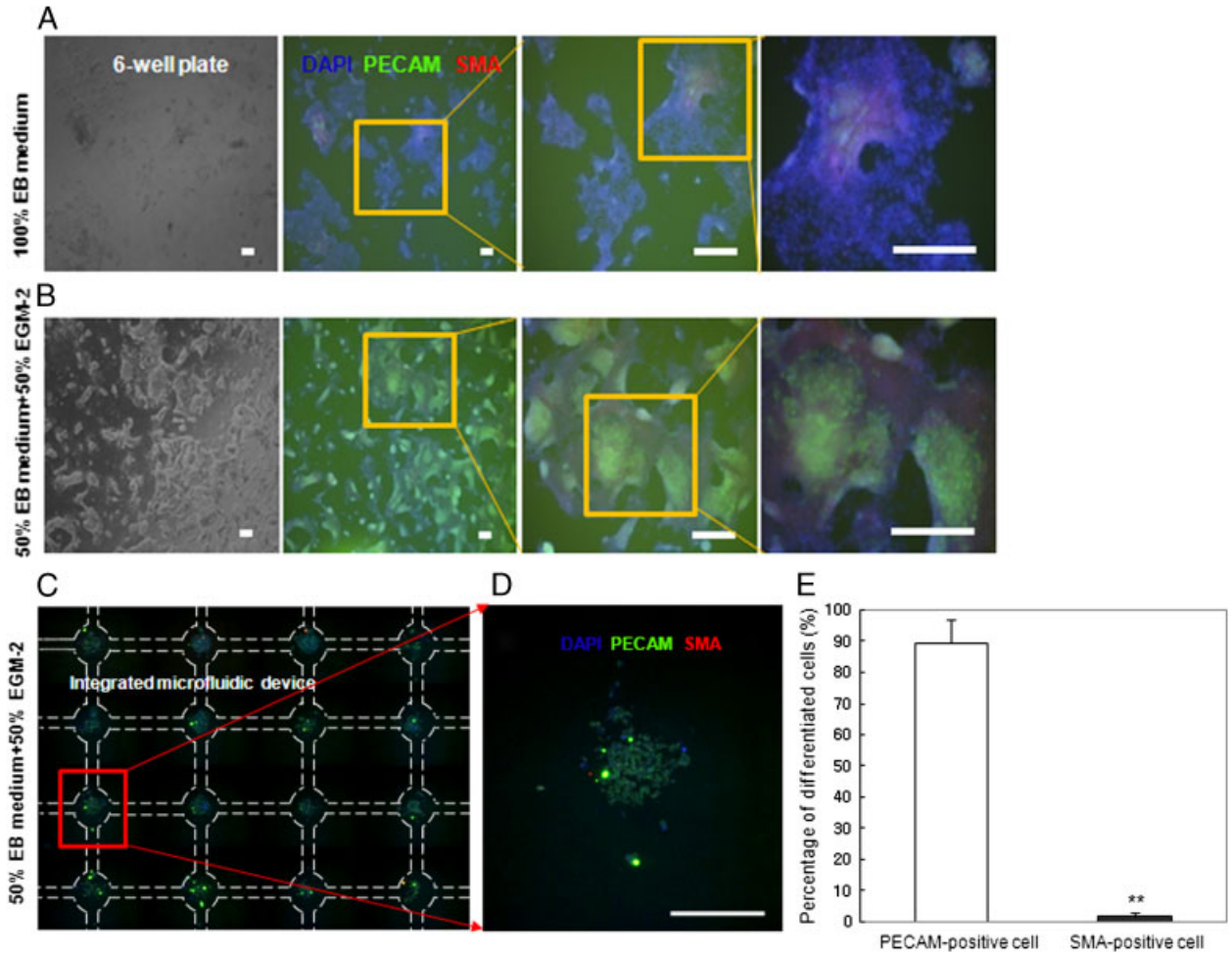

Figure 3. Comparison of ES cell-derived endothelial cell differentiation in a six-well plate and the integrated microfluidic culture device. (A and B) ES cells were cultured with 100% EB medium or 50% EB medium and 50% EGM-2 in a six-well plate. The endothelial cell marker, anti-platelet endothelial cell adhesion molecule (PECAM), is indicated in green and smooth muscle actin (SMA) is indicated in red, respectively. Scale bars are 300 μm. (C and D) In the integrated microfluidic culture device, ES cells were cultured in 50% EB medium and 50% EGM-2 to induce ES cell-derived endothelial cell differentiation. The white dotted lines indicate the microchannel. (E) Quantitative analysis of ES cell-derived endothelial cell differentiation in an integrated microfluidic device. Percentages of differentiated cells indicate the numbers of PECAM- or SMA-positive cells divided by total cell nuclei ($^{**}p < 0.01$). Scale bars are 200 μm.

determine the optimal culture conditions to promote endothelial cell differentiation from ES cells.

In summary, we developed an integrated microfluidic culture device with 4×4 micropillar arrays and microvalves to enable uniform docking of ES cells and medium perfusion. Computational fluid dynamic simulations showed that the velocity and shear stress profiles were strongly affected by the distance between the docking posts within the micropillar arrays. When the distance between the posts was narrow (12 μm), the velocity profiles did not penetrate into the micropillar arrays and shear stress was negligible. We also optimized the flow rate (5–10 μL/min) to achieve uniform ES cell docking within the micropillar arrays. ES cells cultured with 50% EB medium and 50% EGM-2 more differentiated into PECAM-positive endothelial cells. Therefore, this 4×4 integrated microfluidic culture device with shear-protective micropillar arrays is a potentially powerful tool for uniform cell docking and directing ES cell fate.

This paper was supported by a grant from the Korea Healthcare Technology R&D Project, Ministry of Health & Welfare, Republic of Korea (Grant number A100195).

The authors have declared no conflict of interest.

References

[1] Bhattacharya, B., Puri, S., Puri, R. K., *Curr. Stem Cell Res. Ther.* 2009, *4*, 98–106.

[2] Mummery, C., Ward-van Oostwaard, D., Doevendans, P., Spijker, R., van den Brink, S., Hassink, R., van der Heyden,

M., Opthof, T., Pera, M., de la Riviere, A. B., Passier, R., Tertoolen, L., *Circulation* 2003, *107*, 2733–2740.

[3] Kim, J. H., Auerbach, J. M., Rodriguez-Gomez, J. A., Velasco, I., Gavin, D., Lumelsky, N., Lee, S. H., Nguyen, J., Sanchez-Pernaute, R., Bankiewicz, K., McKay, R., *Nature* 2002, *418*, 50–56.

[4] Zhang, S. C., Wernig, M., Duncan, I. D., Brustle, O., Thomson, J. A., *Nat. Biotechnol.* 2001, *19*, 1129–1133.

[5] Poole, T. J., Coffin, J. D., *J. Exp. Zool.* 1989, *251*, 224–231.

[6] Yamashita, J., Itoh, H., Hirashima, M., Ogawa, M., Nishikawa, S., Yurugi, T., Naito, M., Nakao, K., Nishikawa, S., *Nature* 2000, *408*, 92–96.

[7] Vittet, D., Prandini, M. H., Berthier, R., Schweitzer, A., MartinSisteron, H., Uzan, G., Dejana, E., *Blood* 1996, *88*, 3424–3431.

[8] Hwang, Y. S., Chung, B. G., Ortmann, D., Hattori, N., Moeller, H. C., Khademhosseini, A., *Proc. Natl. Acad. Sci. USA* 2009, *106*, 16978–16983.

[9] Zhong, J. F., Chen, Y., Marcus, J. S., Scherer, A., Quake, S. R., Taylor, C. R., Weiner, L. P., *Lab Chip* 2008, *8*, 68–74.

[10] Lii, J., Hsu, W. J., Parsa, H., Das, A., Rouse, R., Sia, S. K., *Anal. Chem.* 2008, *80*, 3640–3647.

[11] Kamei, K., Guo, S., Yu, Z. T., Takahashi, H., Gschweng, E., Suh, C., Wang, X., Tang, J., McLaughlin, J., Witte, O. N., Lee, K. B., Tseng, H. R., *Lab Chip* 2009, *9*, 555–563.

[12] Kang, E., Choi, Y. Y., Jun, Y., Chung, B. G., Lee, S. H., *Lab Chip* 2010, *10*, 2651–2654.

[13] Hung, P. J., Lee, P. J., Sabounchi, P., Lin, R., Lee, L. P., *Biotechnol. Bioeng.* 2005, *89*, 1–8.

[14] Hung, P. J., Lee, P. J., Sabounchi, P., Aghdam, N., Lin, R., Lee, L. P., *Lab Chip* 2005, *5*, 44–48.

[15] Khademhosseini, A., Yeh, J., Eng, G., Karp, J., Kaji, H., Borenstein, J., Farokhzad, O. C., Langer, R., *Lab Chip* 2005, *5*, 1380–1386.

[16] Torisawa, Y. S., Chueh, B. H., Huh, D., Ramamurthy, P., Roth, T. M., Barald, K. F., Takayama, S., *Lab Chip* 2007, *7*, 770–776.

